Mechanism of Inhibition of the GluR2 AMPA Receptor Channel Opening by 2,3-Benzodiazepine Derivatives†

Mark Ritz,‡ Nicola Micale,§ Silvana Grasso,§ and Li Niu*,‡

Department of Chemistry and Center for Neuroscience Research, University at Albany, State University of New York, Albany, New York 12222, and Dipartimento Farmaco-Chimico, Università di Messina, viale Annunziata, 98168 Messina, Italy

Received April 25, 2007; Revised Manuscript Received October 9, 2007

ABSTRACT: 2,3-Benzodiazepine derivatives are drug candidates synthesized for potential treatment of various neurodegenerative diseases involving the excessive activity of AMPA receptors. Here we describe a rapid kinetic investigation of the mechanism of inhibition of the GluR2Q_{flip} AMPA receptor channel opening by two 2,3-benzodiazepine derivatives that are structurally similar (BDZ-2 and BDZ-3). Using a laser-pulse photolysis technique with a time resolution of ∼60 μs, we measured the effects of these inhibitors on both the channel opening rate and the whole-cell current amplitude. We found that both compounds preferably inhibit the open-channel state, although BDZ-2 is a more potent inhibitor in that it inhibits the open-channel state ∼5-fold stronger than BDZ-3 does. Both compounds bind to the same noncompetitive site. Binding of an inhibitor to the receptor involves the formation of a loose, partially conducting channel intermediate, which rapidly isomerizes to a tighter complex. The isomerization reaction is identified as the main step at which the receptor distinguishes the structural difference between the two compounds. These results suggest that addition of a bulky group at the N-3 position on the diazepine ring, as in BDZ-3, does not alter the mechanism of action, or the site of binding, but does lower the inhibitory potency, possibly due to an unfavorable interaction of a bulky group at the N-3 position with the receptor site. The new mechanistic revelation about the structure−reactivity relationship is useful in designing conformation-specific, more potent noncompetitive inhibitors for the GluR2 AMPA receptor.

Glutamate ion channels are classified into three subtypes: *N*-methyl-D-aspartic acid (NMDA), α-amino-3-hydroxy-5-methyl-4-isoxazolepropionic acid (AMPA),[1] and kainate receptors (*1*, *2*). AMPA receptors mediate the majority of fast excitatory neurotransmission in the mammalian central nerve system and are essential in brain activities such as memory and learning (*1*, *2*). Excessive activation of AMPA receptors is, however, known to induce calcium-mediated neurodegeneration, which underlies a variety of acute and chronic neurological disorders, such as post-ischemia cell death, Huntington's chorea, and amyotrophic lateral sclerosis (*2*). Developing AMPA receptor inhibitors to control the excessive receptor activity has been a long-pursued therapeutic approach to the treatment of these neurological disorders (*3*). To make new inhibitors more potent and selective for AMPA receptors, the mechanism of action of existing inhibitors needs to be investigated, and the structure−reactivity relationship for those structurally related compounds needs to be characterized.

2,3-Benzodiazepine derivatives, also known as GYKI compounds, represent one of the best classes of inhibitors in terms of their selectivity and affinity for AMPA receptors. GYKI 52466 [1-(4-aminophenyl)-4-methyl-7,8-methylenedioxy-5*H*-2,3-benzodiazepine] is the first inhibitor in this class discovered in the 1980s (*4*). Since then, hundreds of 2,3-benzodiazepine derivatives have been synthesized (*5*−*7*). GYKI compounds are considered allosteric regulators or noncompetitive inhibitors, a conclusion drawn largely from binding studies using radioactive agonists (*6*). However, the detailed mechanism by which 2,3-benzodiazepines inhibit AMPA receptors is not well documented. This deficiency can be mainly ascribed to the fact that an AMPA receptor opens its channel on the microsecond time scale following glutamate binding (*8*−*10*) but is desensitized or becomes inactivated while glutamate remains bound even on the millisecond time scale (*11*). As a result, the agonist binding assay is most relevant to characterization of the inhibitory effect on desensitized receptors. To assess the channel opening reaction for AMPA receptors, we have previously used a laser-pulse photolysis technique, together with a photolabile precursor of glutamate or the caged glutamate [i.e., *γ*-*O*-(α-carboxy-2-nitrobenzyl)glutamate] (*12*). We have shown that a channel opening reaction can be measured prior to the channel desensitization (*8*, *10*, *13*, *14*).

Here we investigated the mechanism of inhibition of the opening of the GluR2Q_{flip} channel by two 2,3-benzodiazepine compounds, 1-(4-aminophenyl)-3,5-dihydro-7,8-methylenedioxy-4*H*-2,3-benzodiazepin-4-one (BDZ-2) and its 3-*N*-

† This work was supported in part by grants from the Department of Defense (W81XWH-04-1-0106), the ALS Association, and the American Heart Association (0130513T) (to L.N.).

* To whom correspondence should be addressed. Telephone: (518) 591-8819. Fax: (518) 442-3462. E-mail: lniu@albany.edu.

‡ University at Albany, State University of New York.

§ Università di Messina.

[1] Abbreviations: AMPA, α-amino-3-hydroxy-5-methyl-4-isoxazolepropionic acid; BDZ, 2,3-benzodiazepine compounds; GYKI 52466, 1-(4-aminophenyl)-4-methyl-7,8-methylenedioxy-5*H*-2,3-benzodiazepine; caged glutamate, *γ*-*O*-(α-carboxy-2-nitrobenzyl)glutamate; HEK cells, human embryonic kidney cells.

10.1021/bi700782x CCC: $40.75
Published on Web 12/28/2007

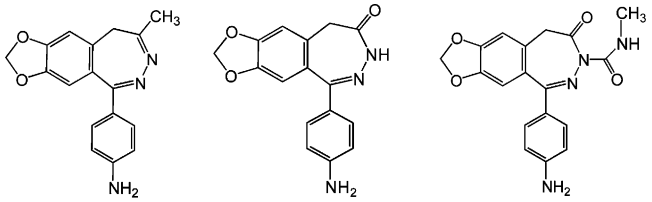

FIGURE 1: Chemical structures of GYKI 52466, BDZ-2, and BDZ-3. The chemical names for these compounds are given in the text.

methylcarbamoyl derivative (BDZ-3) (*15*) (Figure 1). BDZ-2 and BDZ-3 are structurally related to GYKI 52466, a template based on which many derivatives are synthesized (Figure 1). Compared to GYKI 52466, the 4-methyl group is replaced by a carbonyl group in both BDZ-2 and BDZ-3. The $GluR2Q_{flip}$ channel was chosen for this study because the GluR2 subunit in the unedited or Q (glutamine) isoform is known to control the calcium permeability of heteromeric AMPA receptors (*16*, *17*) and is thus considered a key subunit mediating excitotoxicity (*18*). The effect of an inhibitor on the channel opening and channel closing rate constants as well as the whole-cell current amplitude was determined with human embryonic kidney (HEK-293) cells that expressed the $GluR2Q_{flip}$ AMPA channels. Our results show that BDZ-2 and BDZ-3 bind to the same site, and both preferably inhibit the open-channel state of the $GluR2Q_{flip}$ receptor, although BDZ-2 is a stronger noncompetitive inhibitor. Furthermore, the inhibition of the receptor channel by these compounds likely involves the formation of a loose, partially conducting inhibitor−receptor intermediate, which rapidly isomerizes to a tighter, inhibitory complex. The implication of these results on the structure−reactivity relationship for developing more potent, conformation-specific 2,3-benzodiazepine derivatives is discussed.

EXPERIMENTAL PROCEDURES

Cell Culture and Receptor Expression. HEK-293S cells were cultured in Dulbecco's modified Eagle's medium supplemented with 10% fetal bovine serum and in a 37 °C, 5% CO_2, humidified incubator. $GluR2Q_{flip}$ was transiently expressed in these cells using a calcium phosphate method (*8*). HEK-293S cells were also cotransfected with a plasmid encoding green fluorescent protein and a separate plasmid encoding large T-antigen (*19*). The weight ratio of the plasmid for GluR2 to that for green fluorescent protein and large T-antigen was 1:0.2:10, and the $GluR2Q_{flip}$ plasmid used for transfection was ∼5−10 μg/35 mm dish. After 48 h, the transfected cells were used for recording.

Whole-Cell Current Recording. A recording electrode was made from a glass capillary (World Precision Instruments, Sarasota, FL) and had a resistance of ∼3 MΩ when filled with the electrode buffer. The electrode buffer was composed of 110 mM CsF, 30 mM CsCl, 4 mM NaCl, 0.5 mM $CaCl_2$, 5 mM EGTA, and 10 mM HEPES (pH 7.4, adjusted with CsOH). The external buffer contained 150 mM NaCl, 3 mM KCl, 1 mM $CaCl_2$, 1 mM $MgCl_2$, and 10 mM HEPES (pH 7.4, adjusted with NaOH). The whole-cell current was recorded with a cell voltage clamped at −60 mV, using an Axopatch-200B amplifier at cutoff frequency of 2−20 kHz by a built-in, eight-pole Bessel filter, and digitized at a sampling frequency of 5−50 kHz using an Axon Digidata 1322A instrument. The data were acquired using pCLAMP 8 (Molecular Devices, Sunnyvale, CA). All recordings were performed at room temperature. Unless otherwise noted, each data point was the average of at least three measurements collected from at least three cells.

Laser-Pulse Photolysis Measurements. The use of the laser-pulse photolysis technique to measure the channel opening kinetics has been described previously (*8*). Briefly, the caged glutamate (*12*) (Invitrogen, Carlsbad, CA) was dissolved in the external buffer and applied to a cell using a flow device (*20*) (see below). In the laser-pulse photolysis measurement of channel opening, a single laser pulse at 355 nm with a pulse length of 8 ns was generated from a pulsed Q-switched Nd:YAG laser (Continuum, Santa Clara, CA). The pulse energy varied in the range of 200−800 μJ, measured at the end of an optical fiber (300 μm core diameter) to which the laser beam was coupled. To calibrate the concentration of photolytically released glutamate, we applied two solutions of free glutamate with known concentrations to the same cell before and after a laser flash (*9*). The current amplitudes obtained from this calibration were compared with the amplitude from the laser measurement with reference to the dose−response relationship. These measurements also allowed us to monitor any damage to the receptors and/or the cell for successive laser experiments with the same cell (*8*).

To deliver an inhibitor to a cell, we used a "Ψ"-shaped flow device (*21*). The central tubing in the Ψ device was filled with an inhibitor solution for preincubation such that the solution was applied prior to the application of free glutamate as the control or free glutamate but mixed with the same inhibitor at the same concentration. In all experiments reported in this study, a 3 s preincubation flow protocol was required for both BDZ-2 and BDZ-3 to exert full inhibition of the receptor; a preincubation longer than 3 s caused no further current reduction. Furthermore, the 3 s preincuabtion for the ensuing inhibition was independent of glutamate concentration (and thus independent of the receptor form; see the explanation in the text). When the free glutamate was used to induce the receptor response in the absence and presence of an inhibitor, the amplitude of the whole-cell current observed using the flow device was corrected for receptor desensitization by a method previously described (*20*). The corrected current amplitude was used for data analysis.

Experimental Design and Data Analysis. To investigate the mechanism of inhibition, the effects of BDZ-2 or BDZ-3 on the channel opening rate constant (k_{op}) and channel closing rate constant (k_{cl}) were determined. These measurements were carried out at two glutamate concentrations by the following rationale. The observed rate constant (k_{obs}) of $GluR2Q_{flip}$ channel opening is a function of ligand concentration (see eq 2; eq 2 and all other equations are in the Appendix), which includes both rate terms, k_{op} and k_{cl}. This is particularly true experimentally when the molar concentration of ligand or glutamate (L) is either comparable to or larger than the value of the intrinsic equilibrium constant for the ligand (K_1) (*8*). However, when the ligand concentration is lowered (i.e., $L \ll K_1$), the k_{obs} expression or eq 2 is reduced to $k_{obs} \approx k_{cl}$. Under such a condition, the effect of an inhibitor on, and its inhibition constant for, the open-

channel state can be determined (eq 4). At a higher ligand concentration, where $k_{obs} > k_{cl}$, the k_{op} value can be determined from the difference between k_{obs} and k_{cl} or by rearranging eq 2 in that $k_{obs} - k_{cl} = k_{op}[L/(L + K_1)]^2$. Accordingly, the effect of the inhibitor on k_{op} and the inhibition constant for the closed-channel state can be measured (eq 5). Previously, we measured k_{op} and k_{cl} for GluR2Q$_{flip}$ (*8*) and also established the criteria under which k_{cl} can be determined from the measurement of k_{obs} (*8*, *9*). For GluR2Q$_{flip}$, k_{cl} is numerically equal to the k_{obs} obtained at ~100 μM glutamate, which corresponded to ~4% of the fraction of the open-channel form (*8*).

The experimental design of using current amplitude to determine the inhibition constant for both the open-channel and closed-channel states required varying concentrations of glutamate (see eqs 6a and 6b). Specifically, at low glutamate concentrations (i.e., $L \ll K_1$), the majority of the receptor was in the closed-channel state (see Figure 5; defined as the unliganded, singly liganded, and doubly liganded forms). Under this condition, the inhibition constant for the closed-channel state was determined from the ratio of the amplitude (see eqs 6a and 6b). Likewise, at a saturating ligand concentration (i.e., $L \gg K_1$), the majority of the receptor was in the open-channel state. Consequently, the inhibition constant associated with the open-channel state was measured. The basis of using the two ligand concentrations that corresponded to ~4 and ~95% of the open-channel form (*8*) to determine the corresponding inhibition constant was a putative difference in affinity with which a compound inhibited the receptor as a function of agonist concentration. At those very low and very high ligand concentrations (*8*), the apparent inhibition constants were considered pertinent to the closed-channel and open-channel states, respectively.

In double-inhibitor experiments where two inhibitors were used at the same time, the concentration of one inhibitor was kept constant while the concentration of the other was varied (eqs 7 and 8). In these experiments, only the amplitude in the presence (A_I) and absence (A) of two inhibitors was determined. All of the other conditions were the same as described before.

Origin 7 (Origin Lab, Northampton, MA) was used for both linear and nonlinear regressions (Levenberg−Marquardt and simplex algorithms). The error reported refers to the standard error of the fits, unless noted otherwise.

RESULTS

BDZ-2 and BDZ-3 are previously known to inhibit endogenous AMPA receptors in native tissues (*15*). Whether they specifically inhibit the GluR2 AMPA receptor subunit is unclear. Here, we first determined that BDZ-2 and BDZ-3 inhibited the GluR2Q$_{flip}$ receptor, as evidenced, for example, by the reduction of the amplitude of the glutamate-induced whole-cell current via the GluR2 channel in the presence of an inhibitor (Figure 2). At all concentrations of inhibitors and glutamate that were tested, neither inhibitor affected the rate of receptor desensitization, consistent with earlier reports for this class of inhibitors in general (*22*, *23*). We thus focused our investigation of the effect of an inhibitor on both the rate of the channel opening and the maximum current amplitude. For clarity, however, we present experimental data mostly for BDZ-2 since the BDZ-3 data are qualitatively the same.

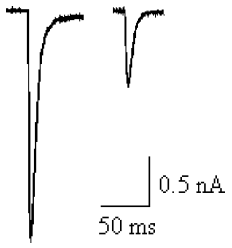

FIGURE 2: Representative whole-cell current traces via GluR2Q$_{flip}$ channels expressed in HEK-293 cells in the absence (left) and presence (right) of BDZ-2. The concentrations of glutamate and the inhibitor were 3 mM and 10 μM, respectively. The whole-cell current was recorded at −60 mV, pH 7.4, and 22 °C.

Effect of BDZ-2 and BDZ-3 on the Channel Opening Rate Constants. The rise of the whole-cell current via the GluR2Q$_{flip}$ channel, initiated by laser photolysis of the caged glutamate, reflected channel opening (Figure 3A) (*8*). As compared to the control, the current rise was slowed and the amplitude was concomitantly reduced in the presence of BDZ-2 (Figure 3A), consistent with the notion that BDZ-2 inhibited the channel opening of GluR2Q$_{flip}$. Furthermore, the observed rate constant in the absence (k_{obs}) and presence of BDZ-2 (k_{obs}') followed a first-order rate expression (eq 1) for ~95% of the rising phase (Figure 3A). Such a monophasic rate process was observed at both 100 ± 10 and 250 ± 20 μM photolytically released glutamate and at all concentrations of either inhibitor, consistent with the assumption that (a) the binding of glutamate and/or inhibitors to the receptor was fast relative to channel opening and (b) the decrease of the rate of channel opening in the presence of inhibitor was a result of receptor inhibition. Furthermore, the rate of desensitization, seen as a current decay (Figure 3A), at any given glutamate concentration in the absence (*8*−*10*, *14*) and presence of an inhibitor at any concentration was at least 10-fold slower than the rate of current rise, suggesting that the channel opening rate could be measured as a distinct kinetic process in the presence of an inhibitor. Thus, the observed rate constant of the channel opening, i.e., k_{obs} or k_{obs}', was calculated (using eq 1) without the complication of desensitization. As such, the mechanism of inhibition of the receptor channel opening (in Figure 5) was formulated without desensitization.

The effects of BDZ-2 on k_{op} and k_{cl} were determined (Figure 3B,C; see also Experimental Procedures for the experimental design). As seen here, BDZ-2 affected k_{cl} (Figure 3B) and k_{op} (Figure 3C). These results indicated that BDZ-2 inhibited both the closed-channel and open-channel states (the inhibition constants for both inhibitors are summarized in Table 1). Our findings are consistent with a noncompetitive inhibition by these compounds (*15*) and suggest that there are regulatory sites to which these inhibitors can bind and inhibit the channel. The effect of BDZ-2 and BDZ-3 on the current amplitude, described below, is also consistent with this conclusion (Table 1).

BDZ-2 and BDZ-3 Inhibited the Channel Opening by a Two-Step Process. We now examine the reduction of the whole-cell current amplitude in the presence of inhibitor. BDZ-2, for instance, reduced the amplitude of the whole-cell response and concurrently slowed the rate of channel opening (Figure 3A). An inhibition constant was calculated from the ratio of the maximum current amplitude in the absence and presence of BDZ-2 as a function of its

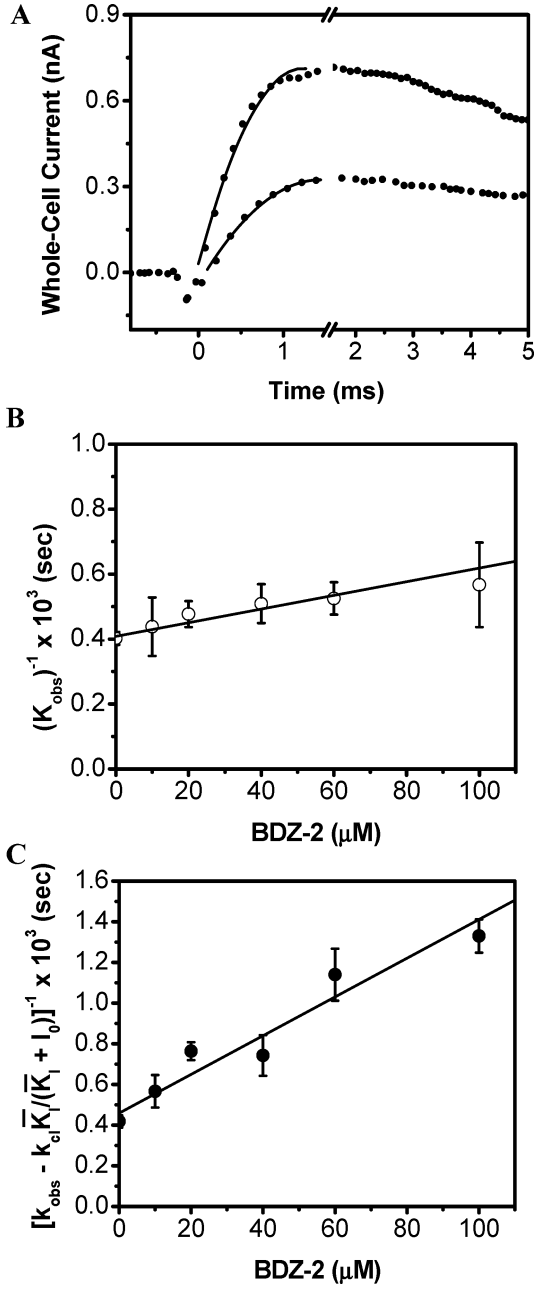

FIGURE 3: Effect of BDZ-2 on the channel opening rate constants. (A) Representative whole-cell current traces from the laser-pulse photolysis experiment showing that BDZ-2 inhibited both the rate and the amplitude of the opening of the GluR2Q_{flip} channel. The top trace is the control (k_{obs} = 2519 s^{-1}; A = 0.70 nA), and the bottom one included 20 μM BDZ-2 (k_{obs} = 2114 s^{-1}; A_I = 0.33 nA). In both traces, the concentration of the photolytically released glutamate was estimated to be 150 μM. (B) Effect of BDZ-2 on k_{cl} obtained at 100 μM glutamate and as a function of BDZ-2 concentration. From this plot, a $\overline{K_I}$* of 194 ± 20 μM was obtained, using eq 4. (C) Effect of BDZ-2 on k_{op} obtained at 250 μM glutamate and as a function of BDZ-2 concentration. From this plot, a K_I^* of 48 ± 5 μM was determined, using eq 5. All of the inhibition constants are summarized in Table 1.

concentration (eq 6 and Figure 4). However, the inhibition constant for both the open-channel and closed-channel states, obtained from the amplitude measurement, was always found to be smaller than the corresponding value obtained from the rate measurement (Table 1). A one-step inhibition model in which the binding of an inhibitor to the receptor directly led to a complete inhibition could not account for this

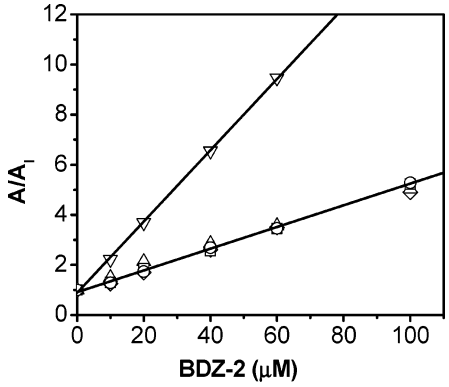

FIGURE 4: Effect of BDZ-2 on the amplitude of the whole-cell current in the absence (A) and presence (A_I) of BDZ-2. An inhibition constant was calculated from this plot using eq 6. At 3 mM glutamate (▽), a $\overline{K_I}$ of 6.9 ± 1.0 μM was obtained, corresponding to the inhibition constant for the open state; a K_I of 24.8 ± 1.0 μM was obtained for the closed-channel state at a glutamate concentration of 100 μM (◇). In both cases, the amplitude was from the flow measurements. From laser-photolysis measurements, a K_I of 25.2 ± 1.0 μM was obtained from the data at 100 μM glutamate and varied concentrations of BDZ-2 (△). At 250 μM glutamate (○), the $\overline{K_I}$ was determined to be 23.0 ± 1.0 μM.

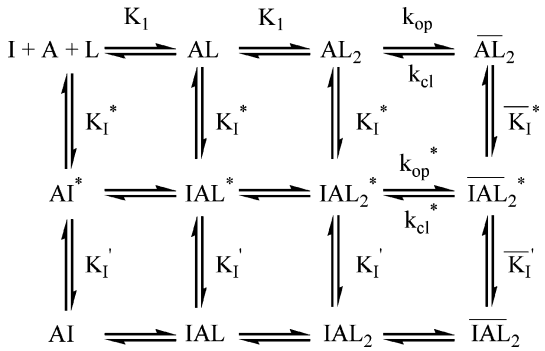

FIGURE 5: Minimal mechanism of the inhibition of the GluR2Q_{flip} receptor by BDZ-2 and BDZ-3 involving an intermediate state. L represents ligand or glutamate, and the number of ligands that bind to and open the channel is assumed to be two (*8*). Here, A represents the active, unliganded form of the receptor, and I represents an inhibitor. For simplicity and without contrary evidence, it is assumed that glutamate binds with equal affinity or K_1, the intrinsic equilibrium dissociation constant, at all binding steps. All the species with an asterisk symbolize those at the intermediate state, whereas those species bound with inhibitor but without an asterisk represent those of the final state. All species related to A, AL, and AL_2, including those bound with inhibitors, are in the closed-channel state, whereas those related to $\overline{AL_2}$ refer to the open-channel state.

discrepancy (*24*). With such a model, the inhibition constant obtained from the rate measurement would be the same as the one obtained from the current amplitude (*24*). However, the discrepancy could be ascribed to a minimal mechanism (in Figure 5) in which the binding of BDZ-2 or BDZ-3 to the receptor initially formed an intermediate (e.g., $\overline{IAL_2}$*) in the first step, and such an intermediate was partially conducting; in the second step, the intermediate isomerized rapidly to form an inhibitory complex ($\overline{IAL_2}$). The two-step inhibition process would apply to both the closed-channel and open-channel states, on the basis of our experimental results (Figure 3B,C).

Using this isomerization model (Figure 5), the discrepancy in the magnitude of the inhibition constant between the rate and the amplitude measurements can now be explained. First,

Table 1: Inhibition Constants of BDZ-2 and BDZ-3, Obtained from Rate and Amplitude Measurements, for the Closed-Channel and Open-Channel States of GluR2Q$_{flip}$

	rate measurement[a]			amplitude measurement		
	K_I^* (μM)[b] (closed channel)	$\overline{K_I}$* (μM)[b] (open channel)	K_I (μM)[b,d]	$\overline{K_I}$ (μM)[b,e]	K_I (μM)[c,d] (closed channel)	$\overline{K_I}$ (μM)[c,f] (open channel)
BDZ-2	48 ± 5	194 ± 20	25.2 ± 1.0	23.0 ± 1.0	24.8 ± 1.0	6.9 ± 1.0
BDZ-3	514 ± 60	204 ± 18	200 ± 18	69 ± 4.0	210 ± 20	38 ± 10

[a] The constants obtained from rate measurements represent those in the first step of inhibition as in Figure 5, whereas those obtained from the amplitude measurements represent the overall inhibition constants. [b] Laser-pulse photolysis measurement. [c] Cell-flow measurement. [d] Measurements at 100 μM glutamate for the closed-channel state. [e] Measurements at 250−350 μM glutamate. [f] Measurements at 3 mM glutamate.

the maximum current amplitude was related to the fraction of the open-channel form at the quasi-equilibrium level, which depended on glutamate concentration (see eq 6b). Therefore, a smaller inhibition constant or a stronger inhibition obtained from the amplitude measurement, as compared with the corresponding inhibition constant from the rate measurement at the same glutamate concentration, suggested that the magnitude of the receptor inhibition obtained from the rate measurement could not account for the total inhibition. An additional step, followed by the formation of the initial, partially conducting receptor−inhibitor intermediate, must be involved to presumably turn the intermediate into a tighter complex, thereby yielding additional inhibition. This assumption is supported by a ratio of inhibition constants being ~28 for the open-channel state (i.e., 194 μM/6.9 μM) in the case of BDZ-2 and a ratio of ~2 for the closed-channel state (i.e., 48 μM/24.8 μM) (in Table 1). BDZ-3 showed a similar, albeit less significant, reduction of the corresponding inhibition constant via the second step (Table 1). Second, a single-exponential current rise for the opening of the channel (Figure 3B) was always observed at all concentrations of the inhibitor (and glutamate), suggesting that the rate constants associated with the two steps in the presence of an inhibitor (Figure 5) were significantly different. If the two rates in the presence of an inhibitor were comparable, a double-exponential rate process would be expected at a certain concentration range of an inhibitor during the whole-cell current rise. Furthermore, the $1/k_{obs}'$ increased linearly with an increase in inhibitor concentration, as predicted by eqs 3−5 derived from one-step inhibition (i.e., the scheme only involving the top and middle rows in Figure 5 with the assumption that the second step is much faster than the first step). Such a linear correlation remained at different glutamate concentrations where the effects of an inhibitor on both k_{cl} and k_{op} were determined (Figure 3B,C). As a result, this linearity allowed us to calculate $\overline{K_I}$* and K* for the intermediate associated with the open channel and closed channel, respectively. If the second step were slow and were measured during the rising phase of the whole-cell current, then the one-step inhibition model should have fully accounted for the inhibition. Consequently, the inhibition constant obtained from the rate measurement would have been identical to the corresponding value obtained from the amplitude measurement (*24*).

Effect of BDZ-2 and BDZ-3 on the Whole-Cell Current Amplitude Determined in Flow Measurements. As an independent approach to evaluation of inhibition constants for both BDZ-2 and BDZ-3 based on the whole-cell current amplitude, we also used a solution flow technique with known concentrations of free glutamate and measured the whole-cell current amplitude in the absence and presence of an inhibitor. The experimental design of using current amplitude to determine the inhibition constants for both the open-channel and closed-channel states required varying concentrations of glutamate (see Experimental Procedures and eqs 6a and 6b). Here, glutamate concentrations from 100 μM to 5 mM were chosen, which corresponded to the fraction of the open-channel form being from ~4 to ~95%, respectively [note that the channel opening probability for this receptor is 96% (*8*)]. The apparent inhibition constants for both BDZ-2 and BDZ-3 were therefore determined at these glutamate concentrations (Figure 4 and Table 1).

Several conclusions can be drawn from these results. First, at a comparable glutamate concentration such as 100 or 250 μM, the A/A_I ratios determined from the flow measurements were identical, within experimental error, to those obtained from the laser-pulse photolysis measurements for both inhibitors (Table 1). Second, at 3 mM glutamate where ~93% of the channels were in the open-channel state, the apparent inhibition constant was considered virtually a measure of the affinity of BDZ-2 for the open-channel state, $\overline{K_I}$, of the GluR2Q$_{flip}$ receptor (see eq 6). Thus, comparison of $\overline{K_I}$ with K_I, the inhibition constant for the closed-channel state, shows that BDZ-2 inhibits the open-channel state ~3.6-fold more strongly (Table 1). BDZ-3, on the other hand, shows a 5-fold stronger inhibition for the open-channel state (Table 1). Third, BDZ-2 is a more potent inhibitor, because it has 5.5- and 8-fold higher affinities for the open-channel and closed-channel states of GluR2Q$_{flip}$, respectively, than BDZ-3 does.

BDZ-2 and BDZ-3 Bind to the Same Inhibitory Site on the GluR2Q$_{flip}$ Receptor. On kinetic grounds (Table 1), BDZ-2 and BDZ-3 share essential functional similarities in that each inhibitor binds to a regulatory (i.e., inhibitory) site on the GluR2Q$_{flip}$ receptor; both inhibit preferentially the open-channel state, although BDZ-2 is a stronger noncompetitive inhibitor. Given the structural similarity between these two compounds (Figure 1), we asked whether they competed for the same regulatory site or bound to two different sites on the receptor. The answer to this question shall have a meaningful implication in improving our understanding of the structure−reactivity relationship of the GYKI compound series, particularly in the prediction of the putative consequence of derivatization at the N-3 position of the diazepine ring.

To address whether the two compounds competed for one inhibitory site or bound separately to two sites, we carried out a double-inhibitor experiment (see Experimental Proce-

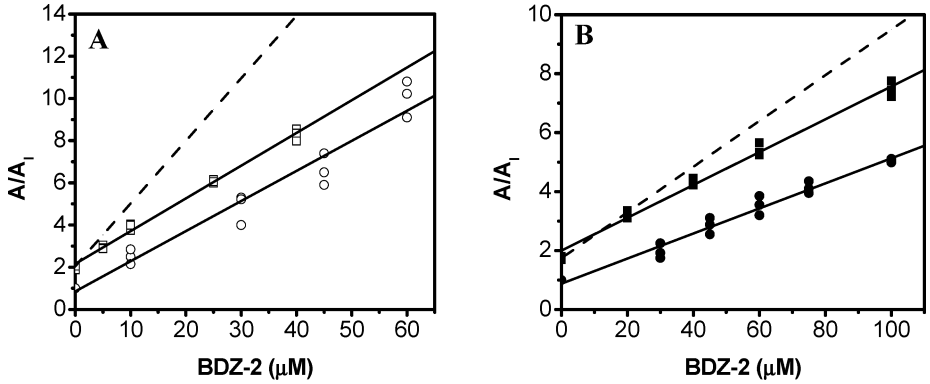

FIGURE 6: Double-inhibition experiments involving both BDZ-2 and BDZ-3. (A) Double inhibition of the open-channel state (3 mM glutamate) of the GluR2Q$_{flip}$ receptor by both BDZ-2 and BDZ-3. The concentration of BDZ-3 was fixed at 40 μM, whereas the concentration of BDZ-2 was varied. The empty circles represent data for BDZ-2 only, and the empty squares represent data for double inhibition by both BDZ-2 and BDZ-3. The K_I of the double inhibition is 6.4 $\pm$ 0.2 μM compared to the value of 6.9 $\pm$ 0.5 μM for just BDZ-2 (Table 1). (B) Double inhibition of the closed-channel state (100 μM glutamate) of the GluR2Q$_{flip}$ receptor by both BDZ-2 and BDZ-3. The concentration of BDZ-3 was fixed at 100 μM, whereas that of BDZ-2 was varied. The filled circles represent data for BDZ-2 only, while the filled squares represent data for both BDZ-2 and BDZ-3. The K_I of the double inhibition was found to be 19.0 $\pm$ 1.0 μM, compared to the K_I of 22.0 $\pm$ 2.0 μM for just BDZ-2 (Table 1). Note that all of the amplitudes used here were from solution-flow measurements. In both panels A and B, the top solid line represents the best fit to the data of the double-inhibition experiments, using eq 7, the one-site model (in the Appendix), compared to the bottom solid line which is the best fit to the data of the single-inhibitor experiment, using eq 6. The dashed line in both panels A and B is the simulated double-inhibition result from eq 8, assuming that the two inhibitors bind to two different sites.

dures and Appendix). The comparison of the ratio of the current amplitude in the absence and presence of two inhibitors with the ratio in the presence of just one inhibitor showed that the slope from which a $K_{I,app}$ value was determined (using eq 7) remained invariant even when the second inhibitor was additionally present (Figure 6). This result suggested that BDZ-2 and BDZ-3 bound to the same site (alternatively, they could bind to two sites, but the binding of the two sites would be mutually exclusive). This conclusion was mutually affirmed from the experiments at two different concentrations of glutamate (Figure 6), which correlated to the open-channel and closed-channel states. Conversely, if BDZ-2 and BDZ-3 bound to two different sites independently, the inhibition would be "additive" or stronger than that of either inhibitor alone, due to an effective increase in the overall concentration of inhibitors bound to the two sites (the dashed line in Figure 6A,B).

DISCUSSION

In this study, we investigated the mechanism of inhibition and the site of interaction for two structurally related inhibitors, BDZ-2 and BDZ-3 (Figure 1). Using the laser-pulse photolysis technique, which previously enabled us to characterize the channel opening rate process of GluR2Q$_{flip}$ (*8*), we measured the effect of each inhibitor on k_{op} and k_{cl} as well as the whole-cell current amplitude. Our findings reveal new features for the mechanism of action and the structure−reactivity relationship of these compounds.

Site of Interaction of BDZ-2 and BDZ-3 with the GluR2Q$_{flip}$ Receptor and Structure−Reactivity Relationship. Both BDZ-2 and BDZ-3 were found to inhibit the GluR2Q$_{flip}$ channel noncompetitively. This conclusion was based on the finding that each of these compounds affected k_{op} and k_{cl}. If BDZ-2, for instance, inhibited the channel uncompetitively, commonly known as open-channel blockade, only the effect on k_{cl}, not that on k_{op}, would be expected; i.e., the $k_{obs} - k_{cl}'$ term in eq 5 would be independent of inhibitor concentration. On the other hand, if BDZ-2 inhibited the channel competitively, only the effect on k_{op}, not that on k_{cl}, would be expected. Furthermore, it is equally important to note that, as observed in both the photolysis and flow measurements, BDZ-2 also inhibited the whole-cell current under the conditions where the open-channel and closed-channel states were measured. Therefore, the effects of BDZ-2 on both the rate constants and the current amplitude are all consistent with the conclusion that BDZ-2 is a noncompetitive inhibitor. The same conclusion can be drawn for BDZ-3.

BDZ-2 and BDZ-3 were also found to compete for the same noncompetitive site on GluR2Q$_{flip}$. Both inhibitors exhibit a higher affinity for the open-channel state of the receptor, although BDZ-2 is a stronger inhibitor. It seems that derivatizing BDZ-2 by addition of a methylcarbamoyl group at the N-3 position of the benzodiazepine ring, resulting in BDZ-3, preserves the same mechanism of action but decreases the overall potency for BDZ-3. One plausible explanation is that the same binding site on the receptor does not prefer to accommodate a bulky group at the N-3 position. We therefore hypothesize that addition of a bulky group at the N-3 position, based on the BDZ-2 template, will yield a compound that prefers to inhibit the open-channel conformation of GluR2Q$_{flip}$ but with a weakened potency.

However, several issues remain. First, the kinetic evidence that enabled us to deduce the site of interaction for BDZ-2 and BDZ-3 with the receptor does not provide the clue for the location of this site (except it is distinct from the agonist binding site). In an attempt to address this question, we performed preliminary NMR experiments using ^{15}N-labeled S1S2 derived from the GluR2Q$_{flip}$ receptor but found no change in chemical shifts when BDZ-2 was mixed with S1S2 (Jayaseelan, Shekhtman, and Niu, unpublished result). One possibility is that the S1S2 protein does not contain the noncompetitive site to which BDZ-2 binds (as a control, mixing of either glutamate or NBQX, a competitive antagonist, with S1S2 did show changes in chemical shifts). A previous study by Balannik et al. (*25*) with a different GYKI compound (i.e., GYKI 53655) suggested that the site of interaction is near the interface between the extracellular binding domain of S1S2 of an AMPA receptor and lipid

bilayer. Balannik and co-workers (*25*) also identified specific amino acid residues affecting the receptor sensitivity to this compound, which are part of the sequences linking the C-termini of S1 and S2 to the transmembrane segments of M1 and M4 or the S1−M1 and S2−M4 regions. However, the linker sequences which cover these residues are not part of the S1S2 construct (*25*). It should be further noted that the C-terminus of S1S2 ends in the middle of the flip-flop region as compared to the full-length receptor (*26*). Taken together, the S1S2 construct is likely incomplete in forming the site for noncompetitive inhibitors, as previously suggested (*25*).

Second, it is not yet known what the structural feature(s) confers the open-channel preferring property to both compounds. What these compounds have in common, as compared with the structure of the parent compound, GYKI 52466 (Figure 1), is the fact that the methyl group at position 4 in the benzodiazepine ring of GYKI 52466 is replaced by a carbonyl group in both BDZ-2 and BDZ-3. Whether this replacement makes a difference in conferring such a preference awaits further study of additional inhibitors, such as GYKI 52466.

Mechanism of Action for BDZ-2 and BDZ-3. Both BDZ-2 and BDZ-3 appear to operate in a two-step process to inhibit the receptor channel. In the first step, an inhibitor forms a loose complex with the receptor, resulting in a partially inhibited channel. In the second step, the intermediate rapidly isomerizes to a tighter complex. This two-step process is evident in a comparison of the inhibition constants associated with the first step and the overall reaction (Table 1). For instance, the inhibition constant for the first step or $\overline{K_I}^*$ is 194 μM for BDZ-2, whereas the overall inhibition constant, $\overline{K_I}$, becomes ~7 μM, reflecting a 28-fold higher potency after an isomerization reaction. This comparison suggests that the initial step, resulting in the formation of an inhibitor−receptor intermediate, is far from sufficient to account for the full inhibition.

However, the incomplete inhibition through the initial inhibitor−receptor channel is unlikely a result of inadequate equilibration of an inhibitor with the receptor site, although a 3 s preincubation was required for a full inhibition. Such a preincubation time would be too long to be considered relevant to a bimolecular rate process for the binding of these compounds to the receptor site in this case. In one scenario that can explain a long preincubation phenomenon for an inhibitor with a fast binding reaction, a slow diffusional access of an inhibitor to its site is required because the site is covered by membrane or is a buried one. Given the results from Balannik et al. (*25*) and our results from a NMR study of the S1S2 binding domain, it is possible that the site to which BDZ-2 and BDZ-3 bind is a buried one. However, in spite of slow diffusional access, subsequent steps can be very fast (but the inhibition can be measured only when the bound activating ligand initiates the channel opening process). On the other hand, if there were a slow inhibitor binding reaction so that the binding could not be treated as a rapid equilibrium on the time scale of channel opening, several phenomena would be anticipated. First, on the time scale of channel opening, we would have measured a bimolecular association reaction, rather than an inhibition reaction. As a result, the observed rate at a fixed glutamate concentration would have been higher as the concentration of inhibitor had increased. However, we observed just the opposite (i.e., k_{obs} was slower when the inhibitor concentration increased). Second, could the binding reaction be so slow that the inhibition occurred on one of the two time scales, both of which were after the channel opening: the inhibition occurred (a) in parallel to the time course for desensitization or (b) after the channel had desensitized or in a second time scale? In both cases, the current amplitude would appear to be smaller or "inhibited" because we would have measured the portion of the receptors without any inhibitors bound. However, neither the desensitization rate nor the rate of channel activity recovery (after the channel was pre-exposed to inhibitor and glutamate) was affected (data not shown); these are the same phenomena reported by Balannik et al. (*25*) for other GYKI compounds. We therefore conclude that the inhibition occurs on the time scale of channel opening, after a full equilibration, consistent with the assumption that the decrease in the rate of channel opening in the presence of an inhibitor was due to inhibition.

Classical examples of a two-step inhibition involving enzyme inhibitors are well documented (*27*, *28*). Mechanisms similar to the one proposed in this study (Figure 5), involving a two-step inhibition process, have also been documented with the muscle nicotinic acetylcholine receptor with several inhibitors (*29*, *30*). For the inhibition of the nicotinic acetylcholine receptor by either cocaine (*29*) or MK-801 (*30*), the first step yields a corresponding channel that is thought to conduct cations as well as or even better than the channel without an inhibitor, thus exhibiting no inhibition on k_{obs} at either a low or a high ligand concentration. In the case of MK-801, the second step, which yields the nonconducting inhibitor−receptor complex, is thought to only occur through the open-channel state (*30*). In the case of BDZ-2 and BDZ-3, a two-step process occurs through both the closed-channel and open-channel states, which is evidenced by the decrease in k_{obs} at both low and high glutamate concentrations.

Implication of Receptor Properties and Structure−Reactivity Relationship. The results of this study (Table 1) reveal new features related to receptor properties and the structure−reactivity relationship for these compounds. The comparison of the overall inhibition constant between BDZ-2 and BDZ-3 shows that BDZ-2 inhibits the open-channel state >5-fold more strongly (see Table 1). However, the inhibition constant for the initial receptor−inhibitor complex for the open-channel state between the two inhibitors is identical [i.e., $\overline{K_I}^*$ is 194 ± 20 μM for BDZ-2 as compared to 204 ± 18 μM for BDZ-3 (Table 1)]. On the other hand, for the closed-channel state, the K_I^* value associated with the initial step for BDZ-2 is already 10-fold different from the value for BDZ-3 (i.e., 48 μM for BDZ-2 vs 514 μM for BDZ-3). Furthermore, when the overall inhibition for the closed-channel state is compared, the difference between BDZ-2 and BDZ-3 is now 8-fold (i.e., 24.8 μM for BDZ-2 vs 210 μM for BDZ-3). This comparison suggests that the isomerization reaction for the *closed-channel state* has merely resulted in ~2-fold improvement for "tightening" the complex for both inhibitors ($\overline{K_I}^*/\overline{K_I}$ = 48/24.8 for BDZ-2 and 514/210 for BDZ-3). In contrast, the receptor−inhibitor complex in the *open-channel state* must undergo an ~5-fold change for BDZ-3 [$\overline{K_I}^*/\overline{K_I}$ = 204/38 (see Table 1)] and

a staggering ~28-fold change for BDZ-2 (i.e., $\overline{K_I}^*/\overline{K_I}$ = 194/6.9). These results thus suggest that the closed-channel state bound with an inhibitor requires less conformational change to become a "tighter" complex than the open-channel state. One possible explanation is that the closed-channel forms are more "accommodating" to binding of inhibitors with different structures and are thus more "modifiable", at least in the first step, than the open-channel form. Our results further suggest that the first step associated with the open-channel state is not the one to distinguish the structural difference between BDZ-2 and BDZ-3, although both compounds preferentially inhibit the open-channel state. Rather, it is the putative isomerization reaction involving the open-channel state that "sees" or discriminates the bulkier side chain at the N-3 position for BDZ-3, resulting in the overall difference in the inhibitory properties between the two compounds. Our results are further consistent with the notion by which, as compared with the initial intermediate, the isomerized receptor−inhibitor complex is tighter, thus making it possible for a closer interaction between the binding site and a binder so that the structural difference between the two inhibitors is distinguished.

Using the rapid kinetic techniques, we show that the mechanism of action and the structure−reactivity relationship of the two 2,3-benzodiazepine derivatives can now be characterized in a more detailed fashion than previously possible. The new findings provide useful clues for the future design and synthesis of 2,3-benzodiazepine inhibitors that are more potent and more specific toward a unique receptor conformation. Our finding that BDZ-3 acts mechanistically the same as BDZ-2 and binds to the same site as BDZ-2 does, but is a weaker inhibitor, indicates that addition of a substituent to the N-3 position on the diazepine ring of BDZ-2, resulting in an increase in size at this position, is expected to generate a weaker inhibitor. However, our finding also suggests a possibility that a photolabel, for instance, can be attached to the N-3 position, and the resulting compound can serve as a site-directed reagent for labeling and mapping of the inhibitory site on the receptor. The location of the site, inferred from this study, is unknown. The location of this and any other regulatory site on any AMPA receptor subunit is in turn beneficial to the design and synthesis of newer 2,3-benzodiazepine derivatives.

APPENDIX

The channel opening rate process of GluR2Q_{flip}, initiated by a laser-pulse photolysis measurement with the caged glutamate, followed a single-exponential rate expression for ~95% of the rise time (*8*). This observation was without exception for all current traces induced by glutamate in the presence and absence of an inhibitor and was therefore consistent with the assumption that the binding of glutamate and/or inhibitor was fast relative to channel opening (*8*). An observed rate constant, k_{obs}, can be calculated from eq 1. In eq 1, I_t represents the current amplitude at time t and I_{max} the maximum current amplitude. Furthermore, using only the upper scheme in Figure 5 or the scheme without any inhibitor bound, k_{obs} can be formulated as in eq 2 to represent the channel opening reaction.

$$I_t = I_{max}(1 - e^{-k_{obs}t}) \quad (1)$$

$$k_{obs} = k_{cl} + k_{op}\left(\frac{L}{L + K_1}\right)^2 \quad (2)$$

When the channel opening rate was inhibited noncompetitively (as in Figure 5), the expression for the observed first-order rate constant was given by eq 3. The derivation of eq 3 was based on the assumption that only the first step was observable (i.e., this step was assigned to the reaction involving the formation of the initial inhibitor−receptor complex) and the second step (i.e., the step leading to the formation of the final receptor−inhibitor complex via a presumed isomerization reaction) was faster than the first step and faster than the rate of channel opening. As such, the effect of an inhibitor on k_{cl} was determined using eq 4, where the inhibition constant associated with the open-channel state ($\overline{K_I}^*$) could be determined (at a low ligand concentration; see the text for further explanation). At higher ligand concentrations, the effect of an inhibitor on k_{op} was determined from the difference between k_{obs} and k_{cl}', as shown in eq 5, and K_I^* was determined (*24*).

$$k_{obs} = k_{cl}\left(\frac{\bar{K}_I^*}{\bar{K}_I^* + I}\right) + k_{op}\left(\frac{L}{L + K_1}\right)^2\left(\frac{K_I^*}{K_I^* + I}\right) \quad (3)$$

$$\frac{1}{k_{obs}} = \frac{1}{k_{cl}} + \frac{1}{k_{cl}}\frac{I}{\bar{K}_I^*} \quad (4)$$

$$(k_{obs} - k_{cl}')^{-1} = [k_{op}L/(L + K_1)^2]^{-1}(1 + I/K_I^*) \quad (5)$$

An inhibition constant was also independently estimated from the ratio of the maximum current amplitudes in the absence, A, and presence, A_I, of an inhibitor, given by eq 6a.

$$\frac{A}{A_I} = 1 + I\frac{(\overline{AL_2})_O}{K_I} \quad (6a)$$

where $(\overline{AL_2})_O$ represents the fraction of the open-channel form and is proportional to the current amplitude. In eq 6b, this fraction is expressed as a function of the fraction of all receptor forms.

$$(\overline{AL_2})_O = \frac{\overline{AL_2}}{A + AL + AL_2 + \overline{AL_2}} = \frac{L^2}{L^2(1 + \Phi) + 2K_1L\Phi + K_1^2\Phi} \quad (6b)$$

Equation 6 permitted the calculation of the apparent overall inhibition constant at a defined agonist concentration. This is especially important for an inhibitor which exhibits a different affinity toward the open-channel and closed-channel states. In that case, the apparent inhibition constant, $K_{I,app}$, is further dependent on the agonist concentration.

To determine whether BDZ-2 and BDZ-3 bound to the same site or two different sites, the two inhibitors were used simultaneously to inhibit the channel activity (*31*). Specifically, the amplitude was measured and used, as in eq 6, to plot $A/A_{I,P}$ versus one inhibitor concentration (see Figure 6). Here, one inhibitor was represented as I while the other was P, all at molar concentrations. Assuming that one inhibitor

bound per receptor and binding of one inhibitor excluded the binding of the other (i.e., one-site model or AI or AP was allowed but not API), the ratio of the current amplitude was given by eq 7 (*31*).

$$\frac{A}{A_{I,P}} = \left(1 + \frac{P}{K_P}\right) + \frac{I}{K_I} \quad (7)$$

On the other hand, for a two-site model in which there were two sites for I and P, respectively (i.e., both AI and AP and API were all allowed), the ratio of the current amplitude was given by eq 8.

$$\frac{A}{A_{I,P}} = \left(1 + \frac{P}{K_P}\right) + \left(1 + \frac{P}{K_P}\right)\frac{I}{K_I} \quad (8)$$

ACKNOWLEDGMENT

We thank Gang Li in the lab for collecting some data on BDZ-3 and Christof Grewer for critical reading of the manuscript.

REFERENCES

1. Hollmann, M., and Heinemann, S. (1994) Cloned glutamate receptors, *Annu. Rev. Neurosci. 17*, 31−108.
2. Dingledine, R., Borges, K., Bowie, D., and Traynelis, S. F. (1999) The glutamate receptor ion channels, *Pharmacol. Rev. 51*, 7−61.
3. Brauner-Osborne, H., Egebjerg, J., Nielsen, E. O., Madsen, U., and Krogsgaard-Larsen, P. (2000) Ligands for glutamate receptors: Design and therapeutic prospects, *J. Med. Chem. 43*, 2609−2645.
4. Tarnawa, I., Farkas, S., Berzsenyi, P., Pataki, A., and Andrasi, F. (1989) Electrophysiological studies with a 2,3-benzodiazepine muscle relaxant: GYKI 52466, *Eur. J. Pharmacol. 167*, 193−199.
5. Zappala, M., Grasso, S., Micale, N., Polimeni, S., and De Micheli, C. (2001) Synthesis and structure-activity relationships of 2,3-benzodiazepines as AMPA receptor antagonists, *Mini-Rev. Med. Chem. 1*, 243−253.
6. Solyom, S., and Tarnawa, I. (2002) Non-competitive AMPA antagonists of 2,3-benzodiazepine type, *Curr. Pharm. Des. 8*, 913−939.
7. Zappala, M., Pellicano, A., Micale, N., Menniti, F. S., Ferreri, G., De Sarro, G., Grasso, S., and De Micheli, C. (2006) New 7,8-ethylenedioxy-2,3-benzodiazepines as noncompetitive AMPA receptor antagonists, *Bioorg. Med. Chem. Lett. 16*, 167−170.
8. Li, G., Pei, W., and Niu, L. (2003) Channel-opening kinetics of GluR2Q_{flip} AMPA receptor: A laser-pulse photolysis study, *Biochemistry 42*, 12358−12366.
9. Li, G., and Niu, L. (2004) How fast does the GluR1Qflip channel open? *J. Biol. Chem. 279*, 3990−3997.
10. Li, G., Sheng, Z., Huang, Z., and Niu, L. (2005) Kinetic mechanism of channel opening of the GluRDflip AMPA receptor, *Biochemistry 44*, 5835−5841.
11. Trussell, L. O., and Fischbach, G. D. (1989) Glutamate receptor desensitization and its role in synaptic transmission, *Neuron 3*, 209−218.
12. Wieboldt, R., Gee, K. R., Niu, L., Ramesh, D., Carpenter, B. K., and Hess, G. P. (1994) Photolabile precursors of glutamate: Synthesis, photochemical properties, and activation of glutamate receptors on a microsecond time scale, *Proc. Natl. Acad. Sci. U.S.A. 91*, 8752−8756.
13. Li, G., Oswald, R. E., and Niu, L. (2003) Channel-opening kinetics of GluR6 kainate receptor, *Biochemistry 42*, 12367−12375.
14. Pei, W., Huang, Z., and Niu, L. (2007) GluR3 flip and flop: Differences in channel opening kinetics, *Biochemistry 46*, 2027−2036.
15. Grasso, S., Micale, N., Zappala, M., Galli, A., Costagli, C., Menniti, F. S., and De Micheli, C. (2003) Characterization of the mechanism of anticonvulsant activity for a selected set of putative AMPA receptor antagonists, *Bioorg. Med. Chem. Lett. 13*, 443−446.
16. Jonas, P., and Spruston, N. (1994) Mechanisms shaping glutamate-mediated excitatory postsynaptic currents in the CNS, *Curr. Opin. Neurobiol. 4*, 366−372.
17. Geiger, J. R., Melcher, T., Koh, D. S., Sakmann, B., Seeburg, P. H., Jonas, P., and Monyer, H. (1995) Relative abundance of subunit mRNAs determines gating and Ca^{2+} permeability of AMPA receptors in principal neurons and interneurons in rat CNS, *Neuron 15*, 193−204.
18. Kwak, S., and Weiss, J. H. (2006) Calcium-permeable AMPA channels in neurodegenerative disease and ischemia, *Curr. Opin. Neurobiol. 16*, 281−287.
19. Huang, Z., Li, G., Pei, W., Sosa, L. A., and Niu, L. (2005) Enhancing protein expression in single HEK 293 cells, *J. Neurosci. Methods 142*, 159−166.
20. Udgaonkar, J. B., and Hess, G. P. (1987) Chemical kinetic measurements of a mammalian acetylcholine receptor by a fast-reaction technique, *Proc. Natl. Acad. Sci. U.S.A. 84*, 8758−8762.
21. Niu, L., Grewer, C., and Hess, G. P. (1996) *Chemical kinetic investigations of neurotransmitter receptors on a cell surface in a microsecond time region*, Vol. VII, Acadamic Press, New York.
22. Donevan, S. D., and Rogawski, M. A. (1993) GYKI 52466, a 2,3-benzodiazepine, is a highly selective, noncompetitive antagonist of AMPA/kainate receptor responses, *Neuron 10*, 51−59.
23. Rammes, G., Swandulla, D., Spielmanns, P., and Parsons, C. G. (1998) Interactions of GYKI 52466 and NBQX with cyclothiazide at AMPA receptors: Experiments with outside-out patches and EPSCs in hippocampal neurones, *Neuropharmacology 37*, 1299−1320.
24. Niu, L., and Hess, G. P. (1993) An acetylcholine receptor regulatory site in BC3H1 cells: Characterized by laser-pulse photolysis in the microsecond-to-millisecond time region, *Biochemistry 32*, 3831−3835.
25. Balannik, V., Menniti, F. S., Paternain, A. V., Lerma, J., and Stern-Bach, Y. (2005) Molecular mechanism of AMPA receptor noncompetitive antagonism, *Neuron 48*, 279−288.
26. Armstrong, N., and Gouaux, E. (2000) Mechanisms for activation and antagonism of an AMPA-sensitive glutamate receptor: Crystal structures of the GluR2 ligand binding core, *Neuron 28*, 165−181.
27. Duggleby, R. G., Attwood, P. V., Wallace, J. C., and Keech, D. B. (1982) Avidin is a slow-binding inhibitor of pyruvate carboxylase, *Biochemistry 21*, 3364−3370.
28. Kulmacz, R. J., and Lands, W. E. (1985) Stoichiometry and kinetics of the interaction of prostaglandin H synthase with anti-inflammatory agents, *J. Biol. Chem. 260*, 12572−12578.
29. Niu, L., Abood, L. G., and Hess, G. P. (1995) Cocaine: Mechanism of inhibition of a muscle acetylcholine receptor studied by a laser-pulse photolysis technique, *Proc. Natl. Acad. Sci. U.S.A. 92*, 12008−12012.
30. Grewer, C., and Hess, G. P. (1999) On the mechanism of inhibition of the nicotinic acetylcholine receptor by the anticonvulsant MK-801 investigated by laser-pulse photolysis in the microsecond-to-millisecond time region, *Biochemistry 38*, 7837−7846.
31. Karpen, J. W., and Hess, G. P. (1986) Cocaine, phencyclidine, and procaine inhibition of the acetylcholine receptor: Characterization of the binding site by stopped-flow measurements of receptor-controlled ion flux in membrane vesicles, *Biochemistry 25*, 1777−1785.

BI700782X